Cell, Vol. 116, 725–736, March 5, 2004, Copyright ©2004 by Cell Press

Nascent Membrane and Secretory Proteins Differ in FRET-Detected Folding Far inside the Ribosome and in Their Exposure to Ribosomal Proteins

Cheryl A. Woolhead,[1,4] Peter J. McCormick,[2] and Arthur E. Johnson[1,2,3,*]
[1]Department of Medical Biochemistry and Genetics
Texas A&M University System Health Science Center
College Station, Texas 77843
[2]Department of Biochemistry and Biophysics
Texas A&M University
College Station, Texas 77843
[3]Department of Chemistry
Texas A&M University
College Station, Texas 77843

Summary

Fluorescence resonance energy transfer measurements reveal that a transmembrane sequence within a nascent membrane protein folds into a compact conformation near the peptidyltransferase center and remains folded as the sequence moves through a membrane bound ribosome into the translocon. This compact conformation is compatible with an α helix because nearly the same energy transfer efficiency was observed when the transmembrane sequence was integrated into the lipid bilayer. Since the transmembrane sequence unfolds upon emerging from a free ribosome, this nascent chain folding is ribosome induced and stabilized. In contrast, a nascent secretory protein is in an extended conformation in the exit tunnel. Furthermore, two ribosomal proteins photocrosslink to nascent membrane but not secretory proteins. These interactions coincide with the previously described sequential closing and opening of the two ends of the aqueous translocon pore, thereby suggesting that ribosomal recognition of nascent chain folding controls the operational mode of the translocon at the ER membrane.

Introduction

In eukaryotic cells, most membrane proteins are synthesized by ribosomes bound to the membrane of the endoplasmic reticulum (ER) at sites termed translocons (for reviews, see Johnson and van Waes, 1999; Schnell and Hebert, 2003). This arrangement allows the nascent proteins to be inserted into the ER membrane as they are being synthesized by the ribosome (cotranslationally). The integration process is mechanically complex because the ribosome and translocon must orient the successive transmembrane sequences (TMSs) of the nascent polypeptide in the membrane to orchestrate the proper delivery of alternating segments of the nascent chain to either the cytoplasmic or the lumenal sides of the membrane. The threading of the nascent protein into the bilayer is further complicated by the fact that the permeability barrier of the membrane must be maintained throughout to avoid the metabolic consequences of unregulated calcium ion release from the ER lumen into the cytoplasm. These superimposed mechanistic demands require the coordinated cooperation of the ribosome, translocon, and other components to successfully achieve membrane protein integration while simultaneously maintaining membrane integrity.

In 1997, Liao et al. identified the sequence of events that maintains the ER membrane permeability barrier during the integration of a single-spanning membrane protein. Since the translocon contains an aqueous pore that spans the membrane (Crowley et al., 1994), one end of the pore must be closed at all times. Several studies have revealed that pore closure is accomplished at its cytoplasmic end by the binding of the ribosome to the translocon (Crowley et al., 1993, 1994; Liao et al., 1997) and at the lumenal end by the action of BiP (Hamman et al., 1998; Haigh and Johnson, 2002; Wirth et al., 2003). During integration of a signal-cleaved membrane protein, the opening and closing of the ends of the pore are controlled by a high-resolution choreography of the translocon, the ribosome, and BiP in different cellular compartments that operate in concert to minimize passive ion diffusion across the membrane (Figure 1A).

Based on the substrate-free crystal structure of an archeal SecYEβ complex, van den Berg et al. (2004) have proposed instead that the translocon pore constricts around a preprotein substrate to prevent ion movement through the channel during translocation and that a translocon contains only a single heterotrimer. Five previous cryo-electron microscopy (cryo-EM) studies cited by van den Berg et al. report that the eukaryotic translocon is multimeric, and hence it is not clear to what extent the archeal crystal structure can be extrapolated to the structure of a ribosome-bound mammalian translocon during translocation, especially since collisional quenching experiments with functional, fully assembled translocation intermediates have shown directly that large ions such as NAD^+ can move through a ribosome-bound translocon pore that is already occupied by a nascent secretory protein (Hamman et al., 1997). One possible explanation for the apparent discrepancy is that in the absence of a preprotein substrate, the archeal SecYEβ crystallizes in a closed monomeric conformation that an individual SecY (or mammalian Sec61α) adopts to maintain the membrane permeability barrier when the protein first enters the bilayer prior to its association with other proteins to form a functional multimeric translocon complex.

The most remarkable aspect of the series of events depicted in Figure 1A is that both BiP binding to the lumenal side of the membrane and the opening of the ribosome-translocon junction occur while the only TMS in the nascent chain is located far inside the ribosome. Thus, it is the ribosome, not the translocon, that first recognizes that the nascent polypeptide is a membrane protein instead of a secretory protein (Liao et al., 1997). This result was very unexpected since it was assumed that the TMS would be recognized only when it reached

*Correspondence: aejohnson@tamu.edu
[4]Present address: GBB, NIDDK, National Institutes of Health, Bethesda, Maryland 20892.

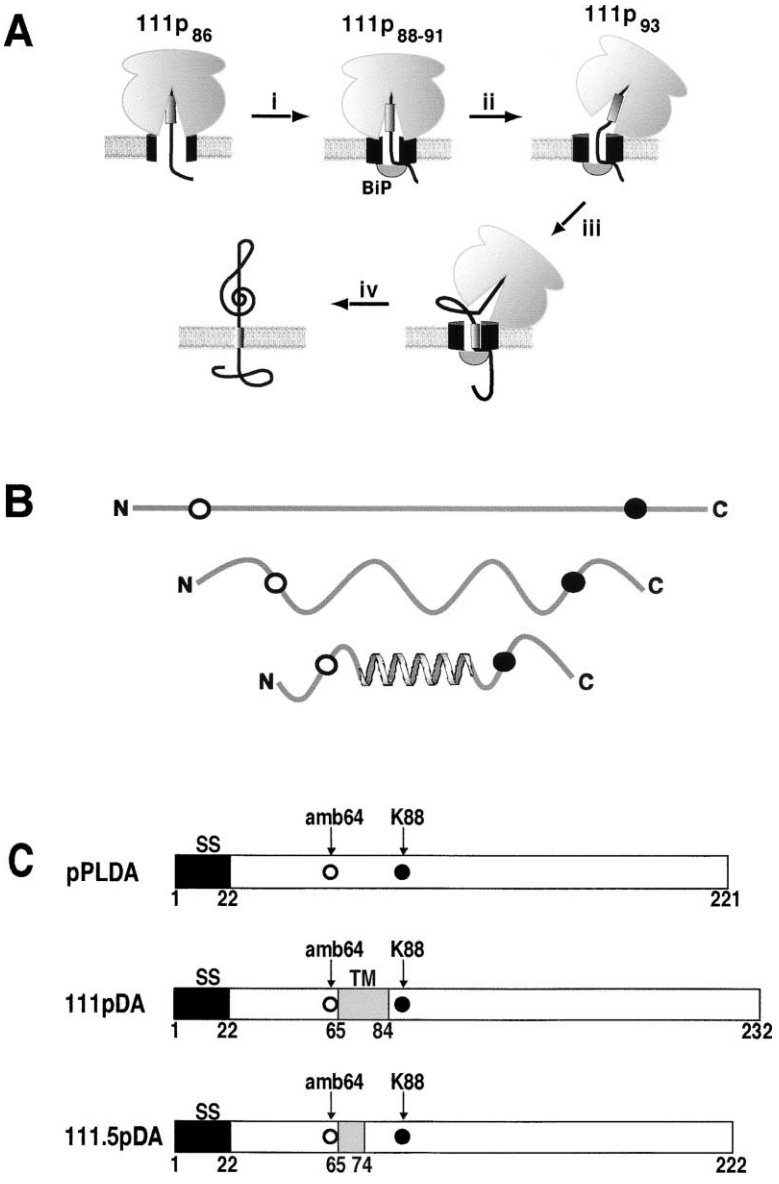

Figure 1. Gating of the Translocon Pore

(A) A RNC containing the nascent single-spanning 111p membrane protein is targeted to the translocon (black) in the ER membrane (gray) by a cleavable signal sequence. When TMS synthesis is complete, the $111p_{86}$ nascent chain is exposed to the ER lumen, but not the cytoplasm (Liao et al., 1997). BiP then seals off (i) the $111p_{88\text{-}91}$ nascent chains from both the cytosol and lumen when the C-terminal end of the TMS is only 4 residues from the PTC. BiP is shown directly plugging the pore, but it may function indirectly via another protein(s) to stimulate pore closure (Haigh and Johnson, 2002). The ion-tight ribosome-translocon junction is opened (ii) in the $111p_{93}$ intermediate to allow the 111p cytoplasmic domain to move into the cytosol (iii) prior to complete integration (iv).

(B) The distance between two fluorescent dyes incorporated into the same polypeptide, and hence the FRET efficiency, will depend upon the structure adopted by the intervening amino acids. Shown top-to-bottom are a fully extended polypeptide, a partially extended polymer, and an α helix. FRET efficiency increases from top-to-bottom as the distance between the probes decreases.

(C) The locations of the single amber stop codon at position 64 and the single lysine codon at position 88 in each DA construct are shown by the open and filled circles, respectively. SS is a cleavable signal sequence (black), while TM indicates the 20 residue VSV-G TMS that includes residues 65 through 84 (gray). In 111.5pDA, the C-terminal half of the 111pDA TMS has been deleted; the remainder is shown in gray.

the translocon. Furthermore, this identification is communicated more than 150 Å across the ER membrane and involves, at a minimum, a ribosomal component, a membrane component, and a lumenal component (Liao et al., 1997; Haigh and Johnson, 2002).

How does the ribosome identify a nascent chain as a membrane protein? The unique feature of every membrane protein is the TMS, a stretch of about 20 mostly nonpolar amino acids. Since BiP-mediated closure of the lumenal end of the pore occurs after the TMS has been synthesized and is located only four amino acids away from the peptidyltransferase center (PTC), Liao et al. (1997) proposed that the ribosome is capable of recognizing a TMS when it is far inside the ribosomal nascent chain exit tunnel. Such recognition would require a means for discriminating between a legitimate TMS and a stretch of nonpolar amino acids that is too short to serve as a TMS (10 residues do not trigger BiP-mediated closure of the pore; Liao et al., 1997). Liao et al. (1997) therefore proposed the existence of a nonpolar patch on the surface of the exit tunnel that would nucleate, via hydrophobic interactions, the folding of a nonpolar stretch in the nascent chain into an α helix. They further suggested that if the putative ribosomal site were sensitive to the length of any helix formed by the nascent chain, then the ribosome could distinguish between TMS and non-TMS hydrophobic sequences. The primary element of this speculative model was therefore a ribosome-induced folding of the nascent chain inside the exit tunnel.

When the high-resolution crystal structure of a large ribosomal subunit was solved three years later, the exit tunnel appeared to have no large nonpolar patches and was barely able to accommodate an α helix at its narrowest point (Nissen et al., 2000). On the other hand, an elongated ribosomal protein, L22, was exposed to both the exit tunnel surface near the PTC and the outer surface of the subunit near the tunnel opening (exit site). This direct structural linkage between the ribosomal and tunnel surfaces made L22 an excellent candidate for a

component of the signaling pathway proposed by Liao et al. (1997).

As for the structural constraints, the experiments of Liao et al. (1997) were done with wheat germ ribosomes, and the exit tunnel in the larger eukaryotic ribosomes may be large enough to accommodate a nascent chain α helix. It is also possible that conformational changes during translation may alter the size of the exit tunnel and/or the exposure of a nonpolar surface to the tunnel. For example, cryo-EM image reconstructions indicate that the size of the entrance to the exit tunnel differs for translating and nontranslating ribosomes (Gabashvili et al., 2001), and another study has shown that the binding of an antibiotic inside the tunnel causes the extended β hairpin loop of L22 to move into the tunnel and block it (Berisio et al., 2003).

The sensitivity of the ribosome to the nascent chain is also shown by its regulation of translation (Tenson and Ehrenberg, 2002). For example, a specific sequence in nascent SecM appears to bind to L22 and/or 23 rRNA at a constriction in the tunnel, thereby stalling translation and stimulating translation of the downstream SecA coding sequence in the mRNA when cellular protein export is insufficient (Nakatogawa and Ito, 2002). Also, TnaC nascent chain interactions within the tunnel can stall translation and thereby regulate the transcription of the tryptophanase operon (Gong and Yanofsky, 2002).

Folding of the nascent chain into a stable tertiary structure inside the exit tunnel would appear to be precluded by its size until the tunnel widens near its exit site (Nissen et al., 2000). Consistent with this view, previous studies of nascent chain folding using a variety of indirect experimental approaches suggest that any tertiary folding starts and proceeds at the distal end of the tunnel near the exit site (reviewed in Kramer et al., 2001). The limited space in the tunnel is also shown by crystal and cryo-EM structures that reveal that macrolide antibiotics bind near the constriction site and block nascent chain egress through the tunnel, thereby blocking translation (Gabashvili et al., 2001; Schlünzen et al., 2001; Hansen et al., 2002; Berisio et al., 2003). On the other hand, some nascent chains appear to form α helices inside the tunnel (Mingarro et al., 2000).

Here we show directly, using fluorescence resonance energy transfer (FRET) between two dyes at defined sites within the same nascent chain, that a TMS in a nascent membrane protein folds into a compact conformation near the PTC. This folding is induced and stabilized by the ribosome, and it persists as the TMS moves down the tunnel, enters the translocon, and inserts into the bilayer. In contrast, a nascent secretory protein is in an extended conformation inside the tunnel. Furthermore, two ribosomal proteins photocrosslink to nascent membrane but not secretory proteins. Taken together, these results suggest a sophisticated mechanism by which the ribosome recognizes nascent membrane proteins and regulates macromolecular interactions on both sides of the ER membrane to accomplish integration while maintaining the permeability barrier.

Results

Experimental Design

FRET is an excellent method for detecting a conformational change and for measuring distances between 20 and 100 Å (Stryer, 1978). The usual FRET experiment requires two fluorescent dyes, each located at a specific site in the same or different molecules. After excitation by the absorption of a photon, the donor dye can transfer its excited state energy to a second chromophore or dye (the acceptor) without the emission of a photon. The efficiency of this transfer depends on, among other things, the extent of overlap of the donor emission and acceptor absorption spectra, the relative orientation of the transition dipoles of the donor and acceptor, and the distance between donor and acceptor dyes. The distance at which the efficiency (E) of energy transfer from the donor to the acceptor is 50% is designated R_0. Since E is equal to $R_0^6/(R_0^6 + R^6)$, E is strongly dependent upon R, the distance separating the donor and acceptor.

To detect whether a nascent chain TMS folds in the exit tunnel, the donor is positioned at one end of the TMS and the acceptor is located at the other end, thereby separating the probes by 24 residues (Figure 1B). If these 24 residues are in an extended conformation, then the two probes will be far apart and have a low FRET efficiency. However, if the intervening 24 residues fold into a more compact conformation such as an α helix, then the probes would be much closer together (residues are separated by 3.5 Å when fully extended and by 1.5 Å along the axis of an α helix) and E would increase dramatically. Thus, we will compare E for two nascent chains in the tunnel, one with the dyes separated by a non-TMS sequence that is predicted to be fully extended (Whitley et al., 1996) and one with the same dyes separated by a TMS that is proposed to fold (Liao et al., 1997) (Figure 1C).

Donor emission intensity is reduced by FRET, and the magnitude of this decrease is used to determine E. Four samples are prepared in parallel that differ only in the presence or absence of the donor and acceptor dyes, and they are designated D (donor-containing), DA(donor- and acceptor-containing), A (acceptor-containing), and B (a blank sample with no donor or acceptor dyes). Subtraction of the B signal from those of D, DA, and A corrects for light scattering and background fluorescence, and subtraction of the net A signal from that of DA corrects for any signal due to direct excitation of the acceptor. E is then calculated most accurately by comparing the net donor emission intensities of the D and DA samples to determine the acceptor-dependent decrease in donor emission. One can also detect FRET by a donor-dependent increase in acceptor emission, but quantifying this increase is more difficult because of the spectral overlap of the donor and acceptor emissions.

The only way to position a probe selectively in the nascent chain in the presence of ribosomes and microsomes is to incorporate the dye into the nascent chain as it is being synthesized by the ribosome. To do this, one requires an aminoacyl-tRNA that recognizes a particular codon, but incorporates an amino acid analog with a fluorescent dye covalently attached to its side chain instead of its natural amino acid. To incorporate two different dyes at specific sites in the nascent chain, two fluorescent-labeled tRNAs with different codon specificities are required, as are mRNAs that contain only one in-frame copy of each of those codons at the desired locations. In this study, ϵBOF-[^{14}C]Lys-tRNA^{Lys} (Experimental Procedures) incorporates the donor at a

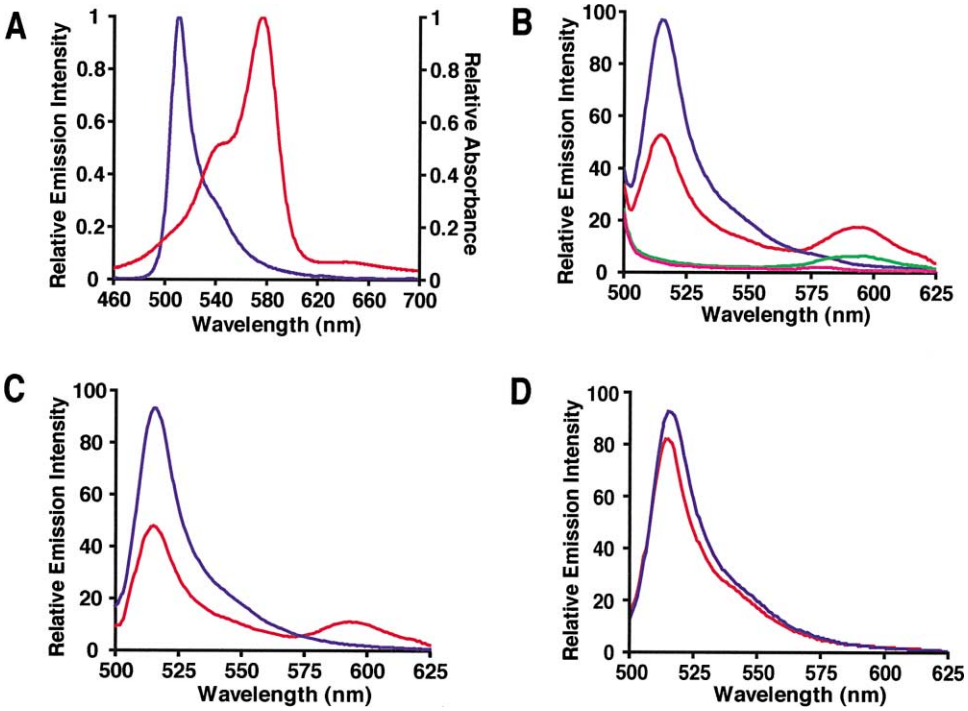

Figure 2. Spectral Characteristics

(A) Spectral overlap. The corrected emission spectrum of the N-hydroxysuccinimidyl ester of BOF (blue) and the absorbance spectrum of the N-hydroxysuccinimidyl ester of BOP (red) in buffer A are shown.

(B) Emission spectra of D (blue), DA (red), A (green), and B (pink) samples containing full-length, membrane-inserted 111pDA are shown. Scans have been normalized as described in Experimental Procedures. These spectra are almost indistinguishable from the corresponding spectra of membrane bound 111pDA RNCs.

(C) Direct comparison of the net emission spectra for the D (blue) and DA (red) samples of Figure 2B after blank subtraction, normalization to the same numbers of dyes, and subtraction of the A spectrum from the DA spectrum.

(D) The blank-subtracted and normalized emission spectra of membrane bound $pPLDA_{90}$ D (blue) and DA (red) samples.

lysine codon in the mRNA and ϵBOP-[^{3}H]Lys-$tRNA^{amb}$ incorporates the acceptor at an amber stop codon.

However, not every lysine and amber codon will incorporate a fluorescent amino acid. Amber suppressor tRNAs ($tRNA^{amb}$) and termination factors compete for every amber stop codon during translation, and about 50% of the nascent chains are typically terminated at an amber stop codon in our samples. Furthermore, Lys-$tRNA^{Lys}$ analogs added to a translation must compete for each lysine codon with endogeneous unmodified Lys-tRNAs, and typically only 25%–30% of the lysines incorporated at a lysine codon under our conditions are modified lysines (Krieg et al., 1989). Thus, the ordering of the lysine and amber codons in the mRNA and of the donor and acceptor dyes in the nascent chain is absolutely critical if one is to do the FRET experiments properly. E can be calculated directly from the net donor emission intensities of the D and DA samples only if every nascent chain with a donor also contains an acceptor. If not, the measured E values must be normalized to account for the fraction of donor-labeled nascent chains that lack an acceptor, and this factor can only be determined by very difficult biochemical and chemical analyses.

To ensure that every nascent chain with a donor also contains an acceptor, one must position the amber stop codon before the lysine codon in the mRNA, and then use a $tRNA^{amb}$ that incorporates the acceptor dye. Every nascent chain that is translated beyond the amber codon will then contain an acceptor; the terminated nascent chains will contain no dyes and will be invisible in our experiments. The donor dye will then be incorporated into only 25%–30% of the nascent chains that are extended beyond the amber codon, but most importantly, every nascent chain with a donor dye will also contain an acceptor dye. Thus, an amber stop codon was introduced at residue 64 and a lysine codon at position 88 in each of three previously characterized constructs (see Experimental Procedures) to create pPLDA and 111.5pDA, two soluble secretory proteins, and 111pDA, a signal-cleaved single-spanning membrane protein containing the TMS of the vesicular stomatitus virus G glycoprotein within the 24 residues that will separate the BOF donor and BOP acceptor (Figure 1C).

Fully assembled translation intermediates with nascent proteins of a defined length were prepared by translating mRNAs that were truncated in the coding region. Ribosomes initiate normally on such mRNAs and translate to the end of the mRNA whenever the amber stop codon is translated by an amber suppressor tRNA in the incubation. The nascent chain then remains bound to the ribosome as a peptidyl-tRNA because there is no other stop codon to effect termination. When transla-

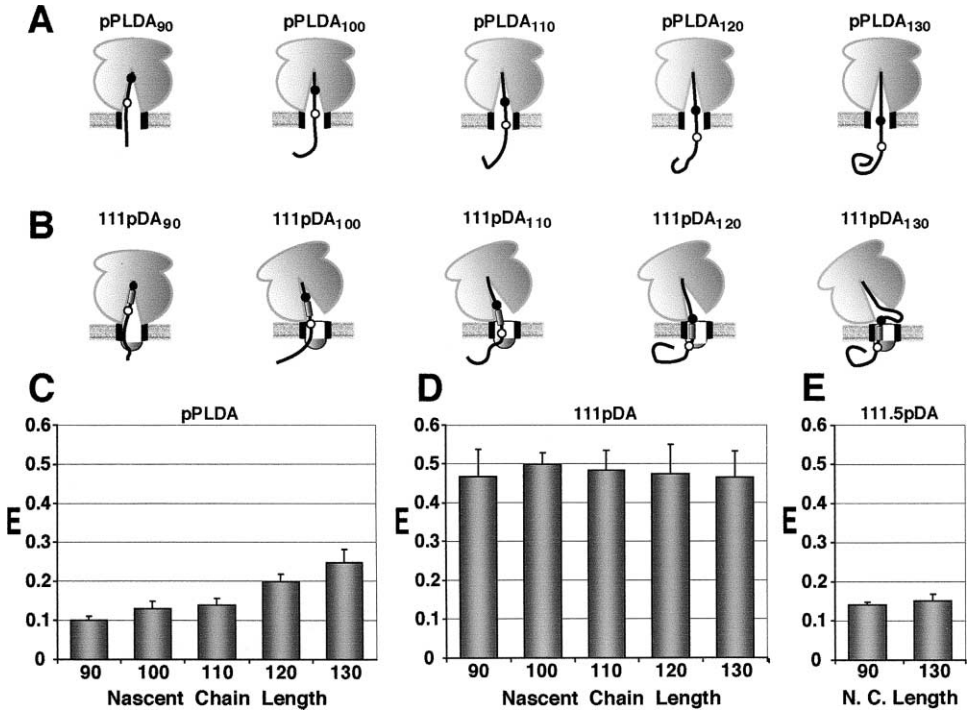

Figure 3. FRET Efficiency in Membrane Bound RNCs

(A) RNCs containing 90, 100, 110, 120, or 130 residue pPLDA nascent chains are shown bound to the translocon. BOF and BOP are indicated by closed and open circles, respectively. Probe positions are estimated assuming that 35 residues are required to span the tunnel and 18 residues are required to span a 50 Å bilayer.

(B) RNCs containing 111pDA nascent chains of the same lengths as in (A) are shown bound to the translocon. The $111pDA_{90}$ pore is sealed on both ends; in the other cases, the lumenal end is closed by BiP and the ribosome-translocon seal is open. The average E values determined for membrane bound pPLDA (C), 111pDA (D), or 111.5pDA (E) RNCs are shown for different lengths of nascent chains. Error bars show the standard deviation of three or more independent experiments.

tions are done in the presence of ER microsomes and signal recognition particles (SRP), ribosome · nascent chain complexes (RNCs) are membrane bound.

pPLDA Is Extended inside the Ribosome

The FRET-detected conformation of a 24 residue segment of a 90 residue pPLDA nascent chain was examined using membrane bound RNCs. D, DA, A, and B samples were prepared in parallel and analyzed spectroscopically to determine E between two probes located 2 and 26 residues from the PTC. Comparison of the net D and DA emission scans for the $pPLDA_{90}$ intermediate (Figure 2D) yielded an average E of 0.10 (Figure 3C), which reveals that the dyes are well separated and hence that this portion of the nascent secretory protein is in an extended conformation inside the tunnel.

Intermediates with longer nascent chains also had low E values when at least one of the probes was inside the ribosome (Figure 3C; the predicted probe locations are shown in Figure 3A). The increase in E observed with $pPLDA_{130}$ indicates that some folding occurs inside the ER lumen because E was only 0.15 in the absence of microsomes.

A TMS Folds inside the Tunnel

When the above FRET experiments were repeated using the 111pDA membrane protein, we obtained dramatically different results. The 111pDA intermediates had the same nascent chain lengths and probe locations as the corresponding pPLDA intermediates (Figure 3B), but the average FRET efficiency was much higher with 111pDA (near 50%; compare Figures 3C and 3D). Typical emission spectra for the 111pDA D, DA, A, and B samples are shown in Figure 2B, and the net emission spectra for the D and DA samples are shown in Figure 2C. It is clear from the latter that the presence of the acceptor greatly decreases the emission intensity of the donor. The net DA spectrum also shows the donor-dependent emission of the acceptor.

The substantially higher E observed with 111pDA than with pPLDA is due almost solely to a decrease in R (see Discussion), which means that BOF and BOP are much closer together in the membrane bound RNCs of 111pDA than of pPLDA. Since these samples differed only in the nascent chain, the sequence that separates the dyes in the two cases must be responsible for the observed difference in E. Thus, whereas the sequence separating BOF and BOP in pPLDA was in an extended conformation, the TMS in 111pDA folded into a compact structure that increased probe proximity. Furthermore, since E was essentially constant as the TMS moved through the tunnel and entered the translocon (Figure 3D), the compact conformation adopted by the TMS was stable.

Ten Nonpolar Residues Do Not Fold inside the Ribosome

If the TMS is responsible for the FRET-detected folding, how many nonpolar residues are required to elicit the

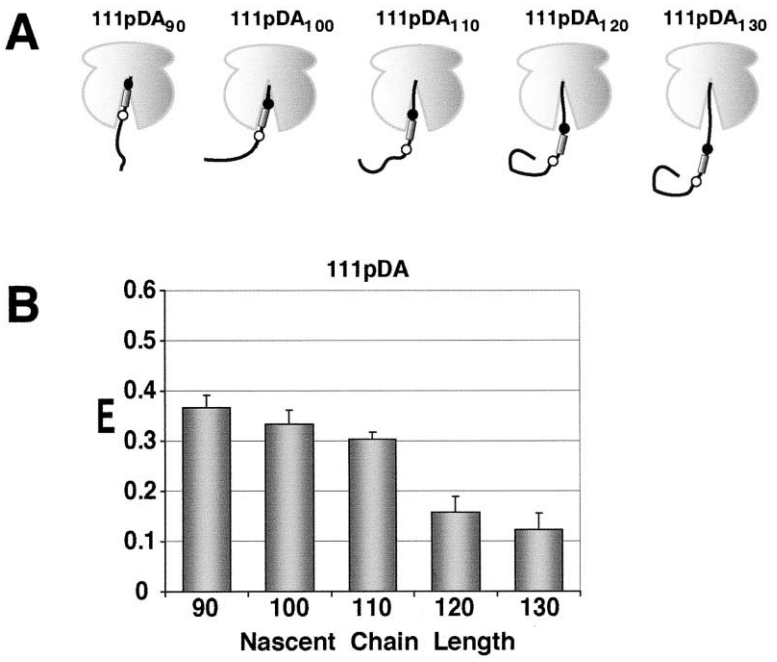

Figure 4. FRET Efficiency in Free 111pDA RNCs

Probe positions and average E values for 111pDA RNCs in the absence of membranes and SRP are shown as in Figure 3.

folding? As a first step in determining this number, we deleted the C-terminal half of the 111pDA TMS without changing the separation of the dyes to form 111.5pDA. When 111.5pDA$_{90}$ and 111.5pDA$_{130}$ intermediates were examined, E was found to be very low (Figure 3E). Thus, a stretch of 10 nonpolar residues was insufficient to trigger the conformational change seen with a 20 residue TMS. Instead, the 24 residue segment between the probes in 111.5pDA adopted an extended conformation very similar to that seen with pPLDA. Hence, the ribosome can apparently distinguish between a legitimate TMS and a long run (10) of nonpolar residues in a soluble nascent protein.

TMS Folding Is Ribosome Induced

Is TMS folding affected by ribosome binding to the translocon? FRET experiments were repeated on the same 111pDA RNCs as above, except that the translations lacked SRP and microsomes. The resulting RNCs were free and not membrane bound (Figure 4A). E was somewhat less for 111pDA$_{90}$ in free than in membrane bound RNCs (Figures 4B and 3D), but was substantially higher than for pPLDA$_{90}$ (Figure 3C). Thus, the TMS in short 111pDA nascent chains folds inside the tunnel whether or not the ribosome is bound to the translocon.

Does the TMS fold spontaneously into a stable compact conformation? Very few polypeptides form α helices by themselves in aqueous solution; most helices are stabilized by associating with or inserting in a nonpolar protein or membrane environment or surface. Here we observed a severe decrease in E when the probes flanking the TMS in 111pDA$_{120}$ both emerged from the ribosome (Figure 4B). Since the spectral parameters (e.g., anisotropy) were the same when the probes were either inside or outside the ribosome (data not shown), the observed decrease in E can only be caused by a significant increase in the distance between the two dyes. Thus, when the TMS leaves the tunnel, its compact conformation is lost and the nascent chain becomes as extended as a non-TMS sequence (E was essentially the same for 111pDA$_{130}$ and pPLDA$_{130}$ in free RNCs; not shown).

FRET Efficiency for a TMS α Helix

The most direct method for determining the E for a TMS α helix is to measure E when the TMS has been integrated into the bilayer and forms a transmembrane α helix (Figure 5A). Full-length 111pDA was synthesized in the presence of SRP and microsomes under conditions that release each TMS into the bilayer (McCormick et al., 2003). From emission spectra (Figure 2), E was determined to be 0.52 for integrated 111pDA (Figure 5B). Consistent with the complete release of full-length 111pDA from ribosomes and translocons, treating samples with puromycin to release residual nascent chains and washing with EDTA to remove ribosomes from the microsomes yielded the same E (not shown). The striking similarity between the E values measured for the full-length inserted protein (Figure 5B) and the nascent chains in membrane bound RNCs (Figure 3D) (the E values are the same within uncertainty, and R differs by only 2 Å) strongly suggests that the compact conformation into which the TMS folds inside the tunnel is an α helix or close to it.

Dye Orientation Effects

κ^2, a geometric factor that depends on the relative orientation of the donor and acceptor dyes, cannot be determined experimentally in a nonrigid system. Thus, R_0 is customarily calculated by assuming that the relative orientation of the donor and acceptor transition dipoles is dynamically randomized during the excited state lifetime of the donor so that $\kappa^2 = 2/3$. This approximation yields values for R that typically differ by less than 10% from those determined by crystallography when such comparisons can be made (e.g., Stryer, 1978; Wu and Brand, 1992; also compare Johnson et al., 1982 with the structure of Yusupov et al., 2001).

However, the theoretical upper and lower limits of κ^2,

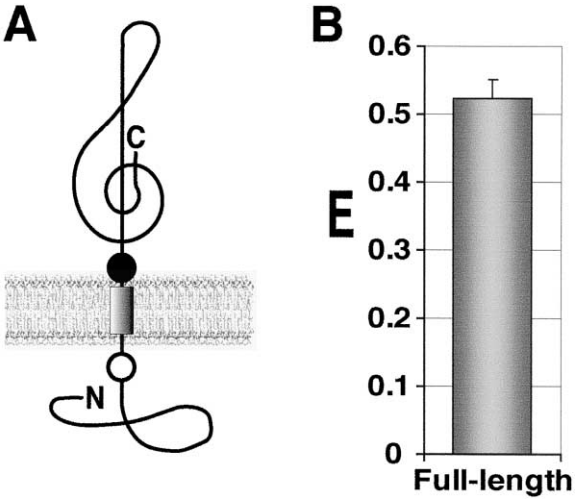

Figure 5. FRET Efficiency for Membrane-Inserted 111pDA

(A) Integration of 111pDA places BOF (●) and BOP (○) on opposite sides of the ER membrane 24 residues apart, 20 of which form a TMS α helix in the bilayer.

(B) E for full-length 111pDA that has been released from the translocon and is embedded in the bilayer.

and hence of R_0, can be determined from anisotropy or polarization data that indicate the freedom of rotation of the dyes in the sample. The measured anisotropy values for BOF (and for BOP) were the same for both free and membrane bound RNCs, for both 111pDA and pPLDA, and for all lengths of nascent chains. For 52 independent measurements of each dye in different samples, the anisotropy was 0.25 ± 0.02 for BOF and 0.30 ± 0.02 for BOP. Each dye therefore has significant freedom of rotation in our samples and is not bound tightly to the ribosome or nascent chain inside the tunnel. This result is not surprising because the dyes are located at the ends of flexible lysine side chains. This conclusion is further supported by the fact that the anisotropy did not change when BOF or BOP moved from inside to outside the tunnel in free RNCs. The above anisotropies yield a maximum range of 0.11 to 3.1 for κ^2 in our samples (Dale et al., 1979). This corresponds to a -25% to $+29\%$ maximum uncertainty in R_0 due to orientational effects. However, as we have discussed and referenced thoroughly in previous studies (Johnson et al., 1982; Watson et al., 1995), the actual uncertainty is closer to 10%, largely because of the statistical improbability of some dye orientations (Hillel and Wu, 1976; Stryer, 1978; Wu and Brand, 1992) and the flexibility of the dye tethers (Wu and Brand, 1992). But most important for the results reported here, one can accurately detect *changes* in the relative location of two dyes by *changes* in E. Thus, the existence of a TMS-dependent difference in E for nascent secretory and membrane proteins reveals important mechanistic aspects of nascent chain folding and the integration process even if the measured distances cannot be precisely related to polypeptide conformation.

Nascent Chain Proximity to Ribosomal Proteins

To ascertain which ribosomal component(s) is (are) involved in distinguishing between nascent secretory and membrane proteins as they move through the tunnel, we determined by photocrosslinking which ribosomal components contact and/or are adjacent to the nascent proteins at different stages of translation. A photoreactive lysine analog was incorporated at residue 75 in each nascent chain to sample its environment approximately halfway between the dye attachment sites. The modified lysine, N^{ϵ}-(5-azido-2-nitro-benzoyl)-Lys (ϵANB-Lys), is not charged, so its presence in the TMS does not interfere with integration (Do et al., 1996; McCormick et al., 2003).

Free RNCs with [^{35}S]Met-labeled pPL-K(75) or 111p(75) nascent chains of various lengths were photolyzed and analyzed by SDS-PAGE. Only one major radioactive band with a higher molecular mass than the nascent chain was observed in the pPL-K samples, so the nascent secretory protein photocrosslinks to a single ribosomal protein with a molecular mass near 40 kDa (Figure 6A, lanes 8–12). In contrast, 111p nascent chains formed three different photoadducts with ribosomal proteins that have apparent molecular masses of about 40, 18, and 7 kDa (Figure 6A, lanes 1–4). It is important to note that since these samples lacked microsomes and SRP, the photocrosslinking targets are all ribosomal in origin. The difference in photoadduct formation shown in Figure 6A reveals that the TMS in nascent 111p membrane proteins is adjacent to two ribosomal proteins that do not contact or are not exposed to nascent pPL-K secretory proteins.

Membrane bound RNCs of 111p and pPL-K exhibited the same photocrosslinking pattern as was observed with the free RNCs (compare Figures 6A and 6B). The photoprobe in the 111p TMS, and hence the TMS itself, was exposed to ribosomal proteins that were not accessible to an equivalent probe in a nascent secretory protein. These gels also showed nascent chain photocrosslinks to both Sec61α and TRAM (identified by immunoprecipitation as in McCormick et al., 2003; data not shown) when the photoprobes in 111p and pPL-K reached the translocon (arrow in Figure 6B, lanes 4–7, 13, 14).

The photocrosslinking of ribosomal proteins to the nascent chain depends upon its length. Both nascent secretory and membrane proteins photocrosslinked to the 40 kDa ribosomal protein when the probe was located 11 amino acids from the PTC, the earliest stage examined here (Figure 6B, lanes 1 and 8). Increasing the pPL-K nascent chain length did not alter its photocrosslinking target (Figure 6B, lanes 8–14). However, extending the 111p nascent chain by 5 amino acids resulted in the appearance of crosslinks to the 18 kDa ribosomal protein (Figure 6B, lane 2). When the 111p nascent chain was lengthened an additional 2 amino acids, significant 111p photocrosslinking to the 7 kDa ribosomal protein was observed in addition to the 18 and 40 kDa photoadducts (Figure 6B, lane 3). The TMS environment therefore changed as it moved through the tunnel.

To ascertain whether the above results were dependent on probe location, we positioned a photoprobe at each of seven different sites within the TMS to scan the proximity of each site to different ribosomal proteins in membrane bound $111p_{86}$, $111p_{91}$, and $111p_{93}$ RNCs. The crosslinking patterns for the seven probe sites in the

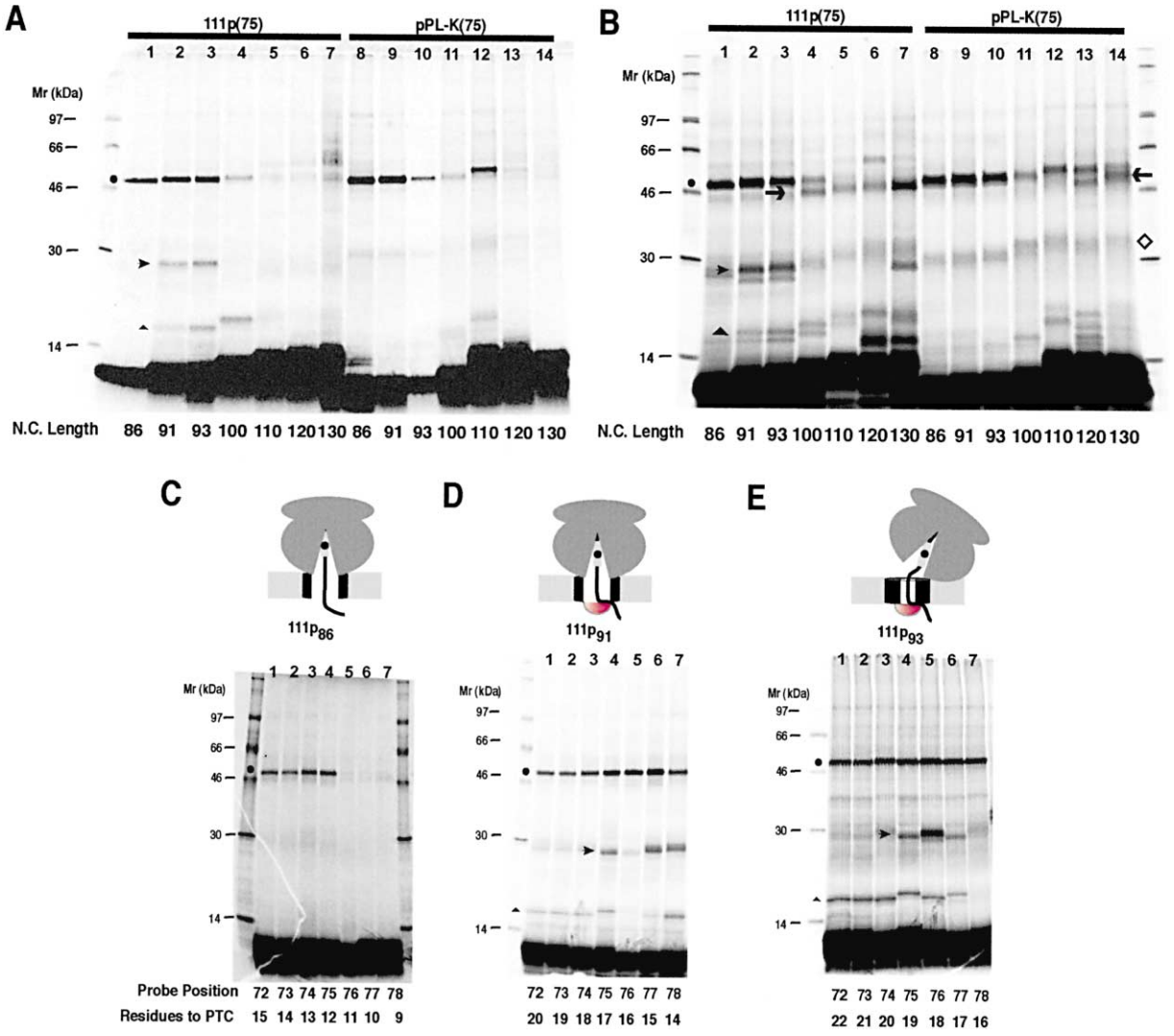

Figure 6. Nascent Chain Exposure to Ribosomal Proteins inside the Exit Tunnel

Free (A) and membrane bound (B) RNCs with ϵANB-Lys probes at position 75 in 111p or pPL-K nascent chains of different lengths were photolyzed and analyzed by SDS-PAGE. Free $111p_{86}$ (C), $111p_{91}$ (D), and $111p_{93}$ (E) RNCs with a single photoprobe in the TMS at the indicated position were photolyzed and analyzed by SDS-PAGE. Nascent chain photoadducts to ribosomal proteins with apparent molecular masses of 40 kDa, 18 kDa, and 7 kDa are indicated by ●, ▶, and ▲, respectively. Photoadducts to Sec61α and TRAM are indicated by ➜. Residual [^{35}S]-labeled peptidyl-tRNAs are responsible for the low-intensity bands identified by the open diamond.

TMS differed markedly for the three intermediates. No crosslinking to the two smaller ribosomal proteins was observed at any probe location for the $111p_{86}$ RNC (Figure 6C). Yet photocrosslinking to the 18 kDa protein occurred from three of the seven probe sites in the TMS in $111p_{91}$ RNCs (Figure 6D). In addition, some weak photocrosslinking to the 7 kDa protein was seen in $111p_{91}$ RNCs (Figure 6D), most notably with the probes located further down the tunnel. In the case of $111p_{93}$ RNCs, ANB at three of seven sites reacted covalently with the 18 kDa protein, and six of seven ANB locations photocrosslinked to the 7 kDa ribosomal protein (Figure 6E).

Most importantly, the pattern of 18 kDa protein photocrosslinking differed for $111p_{86}$, $111p_{91}$, and $111p_{93}$. If the nascent chain were simply sliding past a reactive site in the 18 kDa protein in the tunnel, then one would predict crosslinking to occur from residue n in $111p_{91}$ RNCs and also from residue n + 2 in $111p_{93}$ RNCs. But that is not what happens (compare 73 and 74 in Figure 6D with 75 and 76 in Figure 6E). Thus, nascent chain photocrosslinking to the 18 kDa ribosomal protein is not dictated solely by the location of the probe in the tunnel. Instead, the different photocrosslinking patterns indicate that the ribosome conformation changes during steps i and ii in Figure 1A, thereby altering the position of the 18 kDa ribosomal protein relative to the TMS in the 111p nascent chain. Yet no such conformational change was observed in the absence of the TMS.

Discussion

Several major conclusions are supported by the data reported in this study. First, FRET measurements show

that some nascent chains fold within the exit tunnel. Second, this folding can occur far inside the tunnel and close to the PTC. Third, this folding occurs when the nascent chain contains a TMS, but not when the nascent chain contains a sequence of ten nonpolar residues. Fourth, this folding is ribosome induced and is not stable by itself in aqueous solution. Fifth, the folded conformation is retained as the TMS moves through the tunnel and into the translocon. Sixth, the folded TMS conformation is compatible with an α helix. Seventh, a TMS in the tunnel photocrosslinks to two ribosomal proteins that are not photocrosslinked to a nascent secretory protein, which suggests that these ribosomal proteins are directly involved in the recognition of TMSs and hence nascent membrane proteins.

In addition, TMS proximity to different ribosomal proteins inside the exit tunnel shown here exactly coincides with previously determined changes in nascent chain exposure to the cytoplasmic or lumenal side of the ER membrane. When a RNC forms an ion-tight junction with the cytoplasmic end of the translocon and the pore is open to the ER lumen either during translocation (Crowley et al., 1994) or early in integration (Liao et al., 1997; Haigh and Johnson, 2002; Figure 1A), nascent secretory and membrane proteins photocrosslink only to the 40 kDa ribosomal protein (Figure 6B). But TMS photocrosslinking to the 18 kDa ribosomal protein is detected when the lumenal end of the pore is closed by the action of BiP, and later TMS photocrosslinking to the 7 kDa ribosomal protein is detected when the ribosome-translocon seal is open (Figure 6B; Liao et al., 1997; Haigh and Johnson, 2002). TMS exposure to and/or contact with different ribosomal proteins therefore correlates directly with changes in the structural and functional state of the ribosome-translocon complex. Thus, as proposed by Liao et al. (1997), TMS recognition near the PTC appears to be directly coupled to substantial structural rearrangements on both sides of the membrane.

With regard to the FRET experiments, the observed difference in E for $111pDA_{90}$ and $pPLDA_{90}$ could be caused either by a change in R or by a change in one of the parameters that determine R_0. $R_0^6 = (8.79 \times 10^{-5})QJ_{DA}n^{-4}\kappa^2$, where R_0 is in Å, Q is the quantum yield of the donor in the absence of the acceptor, J_{DA} is the spectral overlap integral, and n is the refractive index of the medium between donor and acceptor. Q and J_{DA} were the same for the pPLDA and 111pDA RNCs (not shown), while changes in n are too small and in the wrong direction to be responsible for the observed change in E. Since the dye anisotropies were the same for both pPLDA and 111pDA, changes in the κ^2 orientation factor could not account for the observed difference in E. Thus, the much higher E observed with 111pDA than with pPLDA is due almost solely to a decrease in the distance between the dyes.

Is the E measured for the integrated TMS reasonable? Since $E = R_0^6/(R^6 + R_0^6)$, the separation between BOF and BOP is 56 Å because R_0 is 57 Å and E is 0.52. BOF and BOP are attached to amino acids separated by approximately 42 Å (19[1.5 Å/helical residue] + 4[3.5 Å/extended residue]) and hence are about 14 Å further apart than the residues to which they are attached. Both BOF and BOP are covalently linked to the polypeptide backbone by lysine side chain tethers that are about 12 Å long when fully extended. Although the dyes could, in principle, sample the space extending 12 Å on all sides of the backbone attachment site, the dyes do not appear to enter the nonpolar core of the bilayer (see below). Instead, the dyes only sample the hemisphere that does not include the membrane interior. Given this restriction, the dyes will, on average, be positioned further from the membrane core than their lysine attachment sites, and 7 Å seems very reasonable for a 12 Å tether.

It is also important to note that the separation between the two dyes is much more than the thickness of the membrane interior. Thus, the dyes are not buried in the bilayer core because their separation would then be less than 30 Å. Instead, the dyes are preferentially located in the interfacial region. Since the dyes do not partition into the hydrophobic membrane core, the dyes are not likely to adsorb to nonpolar ribosomal sites or to the TMS inside the tunnel. This conclusion is fully supported by the anisotropy data and by the long distance separating the dyes in 111pDA RNCs. If BOF and BOP were bound to a nonpolar TMS α-helix inside the tunnel, their separation would be less than 30 Å. The much larger separation measured by FRET indicates that BOP moves ahead of the TMS and BOF follows the TMS in the tunnel. Furthermore, the constancy of E for the various membrane-bound 111pDA RNCs (Figure 3D) reveals that the separation between BOF and BOP does not change significantly ($\pm$ 1 Å) as the TMS moves through the tunnel and into the translocon. This result would not be predicted if either dye were to bind tightly to a site in the tunnel as the nascent chain passed by.

The very low E between two probes positioned 24 residues apart in a nascent secretory protein shows that the probes are separated by a substantial distance in both free (not shown) and membrane bound (Figure 3C) RNCs. Hence, nascent chains lacking a TMS are in an extended conformation as they pass through the exit tunnel. This result is consistent with the conclusions of previous studies (e.g., Whitley et al., 1996). As a nascent secretory protein moves through the tunnel, it passes in close proximity to a 40 kDa ribosomal protein, but apparently is not exposed to two smaller ribosomal proteins (Figure 6). Finally, fluorescence lifetime and collisional quenching experiments show that nascent secretory proteins are in an aqueous environment inside the ribosome and the translocon during translocation and that this aqueous space is contiguous with the ER lumen (Crowley et al., 1994). These nascent chains are not exposed to cytosolic quenching agents because the ribosome forms an ion-tight junction with the translocon that seals off the nascent chain from the cytosol.

In contrast, the high E between two probes positioned at opposite ends of a TMS shows that this portion of a nascent membrane protein folds into a compact conformation almost immediately after the 20 residue TMS is synthesized at the PTC (Figure 3D). Since E was very similar inside the tunnel and when the TMS was fully integrated into the ER membrane (Figures 3D and 5B), the TMS folds into a conformation compatible with an α helix inside the tunnel. Furthermore, the TMS remained folded (retained a high E) as it moved through the ribosome and into the translocon (Figure 3D), but the

TMS was unfolded (had a low E) after emerging from a free ribosome (Figure 4B). The inability of the TMS in 111pDA$_{130}$ to fold in aqueous solution has major ramifications. This result reveals that TMS folding is stabilized by a direct interaction between the nascent chain and the ribosome. Such an interaction most likely involves the association of the nonpolar residues of the TMS with a nonpolar site(s) on the surface of the tunnel that induces the folding of the TMS into a compact structure. Whatever the mechanism, the FRET-detected difference in nascent chain conformation between secretory and membrane proteins is elicited by, and hence is an intrinsic property of, the ribosome because the ribosome-induced change is observed with free ribosomes.

The environment of a TMS also differed from that of a non-TMS inside the ribosome since the TMS was found by photocrosslinking to be adjacent to 18 and 7 kDa ribosomal proteins in addition to a 40 kDa protein (most likely L17, L39, and L4, respectively; see below) (Figure 6). Exposure to these three proteins was staged: 111p$_{86}$ photocrosslinked to L4, but not L17 or L39; 111p$_{91}$ reacted covalently with L4 and L17, but infrequently with L39; and 111p$_{93}$ was adjacent to all three ribosomal proteins (Figures 6C–6E). As noted above, these three different TMS environments correspond to three different structural states for the RNC-translocon complex identified by collisional quenching in which the nascent membrane protein is sealed off, respectively, from the cytosol, from both the cytosol and the lumen, or from the lumen (Liao et al., 1997; Haigh and Johnson, 2002; Figure 1A). This remarkable correlation strongly suggests that the exposure of the folded TMS to L17 results in the BiP-mediated closure of the lumenal end of the translocon pore and that the subsequent exposure of the folded TMS to L39 further down the tunnel elicits the opening of the RNC-translocon seal. Consistent with a major rearrangement of the RNC and translocon relative to each other when the translocon-ribosome junction is opened (Figure 1A), a site in the TMS encounters Sec61α sooner than does the equivalent site in a nascent secretory protein (Figure 6B).

The ribosomal proteins involved in TMS recognition have not been conclusively identified by immunoprecipitation due to the lack of antibodies to the wheat germ proteins. However, Nissen et al. (2000) noted that only three ribosomal proteins were exposed to the tunnel in the H. marismortui large ribosomal subunit crystal structure: L4, L22, and L39e. Since we detect nascent chain photocrosslinking to only three ribosomal proteins in our experiments (Figure 6), it seems likely that the wheat germ ribosomes also have only three proteins exposed to the tunnel. This conclusion is further supported by the fact that we observed the same ribosomal photoadducts and photocrosslinking pattern when 111p(75) was translated in a rabbit reticulocyte lysate (data not shown). The eukaryotic ribosomal proteins that have sequence homology and similar masses to the above H. marismortui proteins are designated L4, L17, and L39 (Ban et al., 2000). Making the reasonable assumption that the three proteins are arranged in equivalent locations in wheat germ, rabbit, and H. marismortui ribosomes, then their locations in the large subunit are very roughly indicated in Figure 7. Both L4 and L17 are elongated, each with a long polypeptide loop that extends from the bulk of the protein at the subunit surface to the tunnel surface near the PTC (Nissen et al., 2000). But whereas L4 is located on the subunit surface near the L1 protuberance, L17 is positioned on the surface very near the exit site where it could interact directly with translocon proteins. Thus, the L17 ribosomal protein that photocrosslinks selectively to a TMS is an excellent candidate for detecting the ribosome-induced folding of the nascent chain TMS with the far end of its β hairpin extension and then undergoing a conformational change that extends to the surface-exposed domain of L17 and an adjacent translocon protein. Alternatively, TMS detection could be communicated by L17 through a more global change in ribosome conformation since H. marismortui L22 directly interacts with portions of all six 23S rRNA domains and hence could effect allosteric changes throughout the subunit (Ban et al., 2000). A transmembrane translocon protein that is sensitive to L17 conformation then presumably elicits the binding

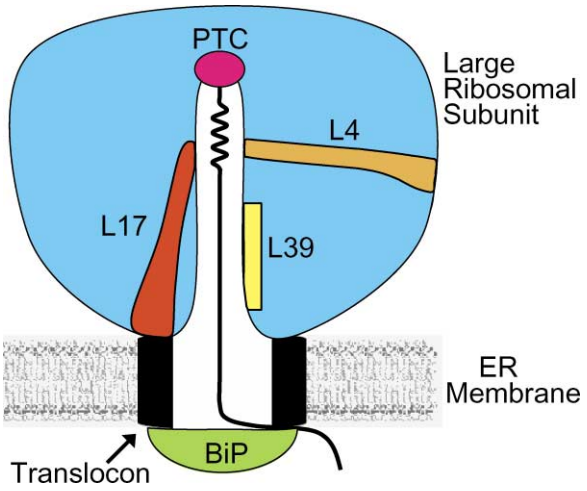

Figure 7. Nascent Chain Control of Ribosome, Translocon, and Lumenal Interactions

The FRET, photocrosslinking, and fluorescence data reveal a remarkable coincidence of TMS folding inside the ribosome, selective nascent membrane protein photocrosslinking to L17 and then L39, and the sequential closing of the lumenal end of the translocon pore and then opening of its cytosolic end. The combined data suggest a likely scenario for ribosome detection of a nascent membrane protein and for transmission of this information to the other side of the membrane. A weakly nonpolar surface in the tunnel formed in part by L17 nucleates the folding of a TMS into a compact conformation compatible with an α helix. The folded TMS elicits a conformational change in L17 that extends to its surface-exposed domain and alters its interaction with a translocon component. The transmembrane translocon protein then undergoes a conformational change that elicits BiP binding and causes the translocon pore to be sealed directly (shown) or indirectly. Upon moving further down the tunnel, the folded TMS interacts with a second ribosomal protein, L39, to elicit the opening of the ribosome-translocon junction (ii in Figure 1A). The molecular components that accomplish the structural changes depicted in Figure 1A (i and ii) have not been conclusively identified, but the mechanism of transmembrane signaling appears to involve a series of nascent chain TMS-dependent conformational changes that involve ribosomal proteins L17 and L39, at least one translocon protein, BiP, and an unknown number of other ribosomal, translocon, and lumenal components.

of BiP and the closure of the pore on the lumenal side of the membrane (Figures 1A and 7). Other than BiP, the number and identities of translocon and lumenal participants in this multicomponent pathway have yet to be determined. Thus, based on these combined data, we propose a sophisticated mechanism by which the ribosome recognizes nascent membrane proteins and then communicates across the ER membrane to maintain the permeability barrier during integration.

Finally, it is important to underscore the technical significance of the approach used here. The successful application of FRET to monitor conformational changes in a specific region of a nascent chain demonstrates that a large number of previously inaccessible questions can now be examined experimentally. For example, the folding (or lack thereof) of both nascent and full-length cytoplasmic, organellar, secretory, and membrane polypeptides can be monitored and characterized, as well as the dependence of their folding on the presence of chaperones, cofactors, and modifying enzymes. Hence, the FRET-based experimental approach reported here has the potential to address a large number of highly significant structural, mechanistic, and regulatory issues in protein folding, processing, assembly, and quality control, among others.

Experimental Procedures

Plasmids, mRNA, and tRNA

R64amb, K75A, and R88K, where "amb" corresponds to the amber stop codon, mutations in the plasmid encoding 111p (Do et al., 1996) yielded 111pDA; R64amb, K75A, and S98K mutations and deletion of residues 75 to 84 in 111p yielded 111.5pDA. K72Q, K78Q, K99Q, S64amb, and C88K mutations in pPL-sK (Crowley et al., 1994) yielded pPLDA. A lysine-free (through residue 130) version of pPL-sK was termed pPL-K. Photocrosslinking experiments were done with an A75K mutation in pPL-K to yield pPL-K(75), and with 111p mutated so as to position a single lysine codon at one of seven sites in the TM sequence. Primary sequences were confirmed by DNA sequencing. Truncated mRNAs were transcribed in vitro using SP6 RNA polymerase and PCR-produced DNA fragments of the desired length (Flanagan et al., 2003).

Lys-tRNA$^{Lys\ or\ amb}$, N$^{\epsilon}$-acetyl-Lys-tRNA$^{Lys\ or\ amb}$ (ϵAc-Lys-tRNA), and ϵANB-Lys-tRNA^{Lys} were prepared as before (Johnson et al., 1976; Krieg et al., 1986; Flanagan et al., 2003). Two BODIPY derivatives were chosen as the donor/acceptor pair because of their high absorptivities, high quantum yields, low spectral sensitivities to their environment, and substantial spectral overlap (Figure 2A). The N-hydroxysuccinimide ester of 4,4-difluoro-5,7-dimethyl-4-bora-3a,4a-diaza-*s*-indacene-3-propionic acid (BODIPY FL, Molecular Probes) was reacted with [^{14}C]Lys-tRNA^{Lys} to form the donor analog ϵBOF-Lys-tRNA^{Lys}, while the N-hydroxysuccinimide ester of 4,4-difluoro-5-(2-pyrrolyl)-4-bora-3a,4a-diaza-*s*-indacene-3-propionic acid (BODIPY 576/589, Molecular Probes) was reacted with [^{3}H]Lys-tRNA^{amb} to form the acceptor analog ϵBOP-Lys-tRNA^{amb}. These reactions were done as in Crowley et al. (1993) except that each 2.5 ml reaction contained 5–6 mg of the BOF or BOP esters, the time at high pH was extended to 25 s, and unreacted dye was removed by repeated ethanol precipitation rather than by benzoylated DEAE-cellulose chromatography.

Translation Intermediates

RNCs were prepared in vitro with truncated mRNAs of 111pDA, 111.5pDA, or pPLDA using wheat germ extract and, for membrane bound RNCs, canine SRP and high salt-washed microsomes (Liao et al., 1997). The translations (26°C, 35 min, 250 μl) differed only in the identity of the added tRNAs (75 pmoles each): DA, ϵBOF-[^{14}C]Lys-tRNA^{Lys} and ϵBOP-[^{3}H]Lys-tRNA^{amb}; D, ϵBOF-[^{14}C]Lys-tRNA^{Lys} and ϵAc-[^{3}H]Lys-tRNA^{amb}; A, ϵAc-[^{14}C]Lys-tRNA^{Lys} and ϵBOP-[^{3}H]Lys-tRNA^{amb}; B, ϵAc-[^{14}C]Lys-tRNA^{Lys} and ϵAc-[^{3}H]Lys-tRNA^{amb}. Substituting ϵAc-Lys for ϵBOF-Lys or ϵBOP-Lys had no significant effect on the number of nascent chains synthesized (not shown). These four samples of membrane bound RNCs were prepared in parallel, incubated in high salt, and purified at 4°C on four separate sepharose CL-2B gel filtration columns (Haigh and Johnson, 2002). RNC samples lacking microsomes were purified at 4°C on four separate sepharose CL-6B gel filtration columns (1.5 cm I.D. $\times$ 18.5 cm) equilibrated in buffer A (50 mM Hepes [pH 7.5], 40 mM KOAc, 5 mM $MgCl_2$). Background light scattering (λ_{ex} = 405 nm, λ_{em} = 420 nm) was equalized for the D, DA, A, and B samples by dilution as necessary prior to initiating fluorescence measurements (Crowley et al., 1994).

Spectral Measurements

Steady-state and time-resolved fluorescence measurements were made with an SLM-8100 or ISS Model K2-002 spectrofluorometer and analyzed as before (Crowley et al., 1993). All measurements were done at 4°C in buffer A using 4 $\times$ 4 mm quartz cuvettes and a bandpass of 4 nm in the SLM; in each case, including anisotropy, the signal of the B sample was subtracted from the signals of the D, DA, and A samples prior to any further analysis.

Eight emission scans (λ_{ex} = 485 nm, λ_{em} = 500–625 nm) were typically averaged for each measurement. The spectral overlap integral, J_{DA}, was determined to be 2.31 $\times$ 10^{15} $M^{-1}cm^{-1}nm^4$ from the corrected BOF emission spectrum, the BOP absorbance spectrum, and a BOP extinction coefficient of 83,000 $M^{-1}cm^{-1}$ at 575 nm (Mutucumarana et al., 1992). Since the BOF and BOP spectra were the same for free, tRNA bound, and nascent chain-incorporated dyes, J_{DA} was not sensitive to dye environment. Steady-state anisotropy was determined as before (Mutucumarana et al., 1992) using λ_{ex} and λ_{em} of 485 and 515 nm for BOF and 575 and 595 nm for BOP. The BOF fluorescence lifetime was determined as before (Crowley et al., 1993) to be 5.6 $\pm$ 0.2 ns for both ϵBOF-Lys-tRNA and ϵBOF-Lys incorporated into RNCs.

Q for the free BOF dye was determined experimentally (Mutucumarana et al., 1992) to be 0.95 in buffer A using disodium fluorescein in 0.1 M NaOH as the standard (Q = 0.92; Weber and Teale, 1957). λ_{ex} was 460 nm, and the corrected emission intensities were integrated from 480 to 700 nm. Since the BOF fluorescence lifetime was unchanged by incorporation into RNCs, its quantum yield in RNCs was taken to be 0.95. Using the equation and data given above, R_0 was determined to be 57 Å by assuming that n is 1.4 (Johnson et al., 1982) and κ^2 is 2/3.

F_D, F_{DA}, and F_A are the net (after F_B subtraction) emission intensities of the D, DA, and A samples at 515 nm (BOF $\lambda_{em\ max}$). The number of dyes in each sample was determined directly by quantifying its ^{14}C and ^{3}H content using the experimentally determined counting efficiencies of 0.60 and 0.16 for ^{14}C and of 0.0 and 0.40 for ^{3}H in the double-label settings of a liquid scintillation counter. F_D was then normalized to the same number of donor dyes as in F_{DA} (ϵBOF-Lys-tRNA preparations contained less than 1% Lys-tRNA), and F_A was normalized to the same number of acceptor dyes as in F_{DA}. Since BOP is too far from BOF to alter its absorbance, E was then given by $E = 1 - (Q_{DA}/Q_D) = 1 - (F_{DA} - F_A)/F_D$. The absolute value of E provides a direct measure of the separation between the dyes, but the uncertainties associated with these measurements (e.g., κ^2 and the lengths of the probe-to-nascent chain tethers) preclude a definitive determination of the actual polypeptide conformation. Our goal was therefore not to measure an absolute distance, but rather to determine whether or not probe separation was altered by the presence of a TMS in the nascent chain.

Photocrosslinking

In vitro translations (50 μl, 26°C, 30 min) containing 32 pmoles of ϵANB-Lys-tRNA^{Lys}, 50 μCi of [^{35}S]Met, and (where indicated) 40 nM SRP and 16 equivalents of column-washed microsomes were performed in the dark as before (McCormick et al., 2003) with truncated pPL-K or 111p mRNAs containing a single Lys codon as indicated. Membrane bound RNCs were photolyzed and analyzed by immunoprecipitation and/or SDS-PAGE as before. After photolysis, free RNCs were sedimented through a sucrose cushion (130 μl; 0.5 M sucrose, 25 mM Hepes [pH 7.5], 130 mM KOAc, 3 mM $Mg[OAc]_2$)

in a Beckman TLA-100 rotor (100,000 rpm, 10 min, 4°C) and resuspended in 50 μl of 50 mM Hepes, 6 mM EDTA at pH 7.5. All samples were treated with RNase A (1 μg, 26°C, 10 min) to remove residual peptidyl-tRNA before the addition of sample buffer.

Acknowledgments

We thank Y. Miao and Y. Shao for excellent technical assistance and Dr. A. Heuck for lifetime measurements. This work was supported by NIH grant GM 26494 and the Robert A. Welch Foundation.

Received: September 24, 2003
Revised: January 13, 2004
Accepted: January 20, 2004
Published: March 4, 2004

References

Ban, N., Nissen, P., Hansen, J., Moore, P.B., and Steitz, T.A. (2000). The complete atomic structure of the large ribosomal subunit at 2.4 Å resolution. Science *289*, 905–920.

Berisio, R., Schlünzen, F., Harms, J., Bashan, A., Auerbach, T., Baram, D., and Yonath, A. (2003). Structural insight into the role of the ribosomal tunnel in cellular regulation. Nat. Struct. Biol. *10*, 366–370.

Crowley, K.S., Reinhart, G.D., and Johnson, A.E. (1993). The signal sequence moves through a ribosomal tunnel into a noncytoplasmic aqueous environment at the ER membrane early in translocation. Cell *73*, 1101–1115.

Crowley, K.S., Liao, S., Worrell, V.E., Reinhart, G.D., and Johnson, A.E. (1994). Secretory proteins move through the endoplasmic reticulum membrane via an aqueous, gated pore. Cell *78*, 461–471.

Dale, R.E., Eisinger, J., and Blumberg, W.E. (1979). The orientational freedom of molecular probes. The orientation factor in intramolecular energy transfer. Biophys. J. *26*, 161–194.

Do, H., Falcone, D., Lin, J., Andrews, D.W., and Johnson, A.E. (1996). The cotranslational integration of membrane proteins into the phospholipid bilayer is a multistep process. Cell *85*, 369–378.

Flanagan, J.J., Chen, J.-C., Miao, Y., Shao, Y., Lin, J., Bock, P.E., and Johnson, A.E. (2003). Signal recognition particle binds to ribosome-bound signal sequences with fluorescence-detected subnanomolar affinity that does not diminish as the nascent chain lengthens. J. Biol. Chem. *278*, 18628–18637.

Gabashvili, I.S., Gregory, S.T., Valle, M., Grassucci, R., Worbs, M., Wahl, M.C., Dahlberg, A.E., and Frank, J. (2001). The polypeptide tunnel system in the ribosome and its gating in erythromycin resistance mutants of L4 and L22. Mol. Cell *8*, 181–188.

Gong, F., and Yanofsky, C. (2002). Instruction of translating ribosome by nascent peptide. Science *297*, 1864–1867.

Haigh, N.G., and Johnson, A.E. (2002). A new role for BiP: Gating the aqueous ER translocon pore during membrane protein integration. J. Cell Biol. *156*, 261–270.

Hamman, B.D., Chen, J.-C., Johnson, E.E., and Johnson, A.E. (1997). The aqueous pore through the translocon has a diameter of 40-60 Å during co-translational protein translocation at the ER membrane. Cell *89*, 535–544.

Hamman, B.D., Hendershot, L.M., and Johnson, A.E. (1998). BiP maintains the permeability barrier of the ER membrane by sealing the lumenal end of the translocon pore before and early in translocation. Cell *92*, 747–758.

Hansen, J.L., Ippolito, J.A., Ban, N., Nissen, A., Moore, P.B., and Steitz, T.A. (2002). The structures of four macrolide antibiotics bound to the large ribosomal subunit. Mol. Cell *10*, 117–128.

Hillel, Z., and Wu, C.-W. (1976). Statistical interpretation of fluorescence energy transfer measurements in macromolecular systems. Biochemistry *15*, 2105–2113.

Johnson, A.E., and van Waes, M.A. (1999). The translocon: a dynamic gateway at the ER membrane. Annu. Rev. Cell Dev. Biol. *15*, 799–842.

Johnson, A.E., Woodward, W.R., Herbert, E., and Menninger, J.R. (1976). N^{ϵ}-acetyllysine transfer ribonucleic acid: A biologically active analogue of aminoacyl transfer ribonucleic acids. Biochemistry *15*, 569–575.

Johnson, A.E., Adkins, H.J., Matthews, E.A., and Cantor, C.R. (1982). Distance moved by transfer RNA during translocation from the A site to the P site on the ribosome. J. Mol. Biol. *156*, 113–140.

Kramer, G., Ramachandiran, V., and Hardesty, B. (2001). Cotranslational folding - omnia mea mecum porto? Int. J. Biochem. Cell Biol. *33*, 541–553.

Krieg, U.C., Walter, P., and Johnson, A.E. (1986). Photocrosslinking of the signal sequence of nascent preprolactin to the 54-kilodalton polypeptide of the signal recognition particle. Proc. Natl. Acad. Sci. USA *83*, 8604–8608.

Krieg, U.C., Johnson, A.E., and Walter, P. (1989). Protein translocation across the endoplasmic reticulum membrane: identification by photocross-linking of a 39 kD integral membrane glycoprotein as part of a putative translocation tunnel. J. Cell Biol. *109*, 2033–2043.

Liao, S., Lin, J., Do, H., and Johnson, A.E. (1997). Both lumenal and cytosolic gating of the aqueous ER translocon pore is regulated from inside the ribosome during membrane protein integration. Cell *90*, 31–41.

McCormick, P.J., Miao, Y., Shao, Y., Lin, J., and Johnson, A.E. (2003). Cotranslational protein integration into the ER membrane is mediated by the binding of nascent chains to translocon proteins. Mol. Cell *12*, 329–341.

Mingarro, I., Nilsson, I., Whitley, P., and von Heijne, G. (2000). Different conformations of nascent polypeptides during translocation across the ER membrane. BMC Cell Biol. *1*, 3.

Mutucumarana, V.P., Duffy, E.J., Lollar, P., and Johnson, A.E. (1992). The active site of factor IXa is located far above the membrane surface and its conformation is altered upon association with factor VIIIa. A fluorescence study. J. Biol. Chem. *267*, 17012–17021.

Nakatogawa, H., and Ito, K. (2002). The ribosomal exit tunnel functions as a discriminating gate. Cell *108*, 629–636.

Nissen, P., Hansen, J., Ban, N., Moore, P.B., and Steitz, T.A. (2000). The structural basis of ribosome activity in peptide bond synthesis. Science *289*, 920–930.

Schlünzen, F., Zarivach, R., Harms, J., Bashan, A., Tocilj, A., Albrecht, R., Yonath, A., and Franceschi, F. (2001). Structural basis for the interaction of antibiotics with the peptidyl transferase centre in eubacteria. Nature *413*, 814–821.

Schnell, D.J., and Hebert, D.N. (2003). Protein translocons: multifunctional mediators of protein translocation across membranes. Cell *112*, 491–505.

Stryer, L. (1978). Fluoresence energy transfer as a spectroscopic ruler. Annu. Rev. Biochem. *47*, 819–846.

Tenson, T., and Ehrenberg, M. (2002). Regulatory nascent peptides in the ribosomal tunnel. Cell *108*, 591–594.

van den Berg, B., Clemons, W.M., Jr., Collinson, I., Modis, Y., Hartmann, E., Harrison, S.C., and Rapoport, T.A. (2004). X-ray structure of a protein-conducting channel. Nature *427*, 36–44.

Watson, B.S., Hazlett, T.L., Eccleston, J.F., Davis, C., Jameson, D.M., and Johnson, A.E. (1995). Macromolecular arrangement in the aminoacyl-tRNA•elongation factor Tu•GTP ternary complex. A fluorescence energy transfer study. Biochemistry *34*, 7904–7912.

Weber, G., and Teale, F.W.J. (1957). Determination of the absolute quantum yield of fluorescent solutions. Trans. Faraday Soc. *53*, 646–655.

Whitley, P., Nilsson, I., and von Heijne, G. (1996). A nascent secretory protein may traverse the ribosome/endoplasmic reticulum translocase complex as an extended chain. J. Biol. Chem. *271*, 6241–6244.

Wirth, A., Jung, M., Bies, C., Frien, M., Tyedmers, J., Zimmermann, R., and Wagner, R. (2003). The Sec61p complex is a dynamic precursor activated channel. Mol. Cell *12*, 261–268.

Wu, P., and Brand, L. (1992). Orientation factor in steady-state and time-resolved resonance energy transfer measurements. Biochemistry *31*, 7939–7947.

Yusupov, M.M., Yusupova, G.Z., Baucom, A., Lieberman, K., Earnest, T.N., Cate, J.H.D., and Noller, H.F. (2001). Crystal structure of the ribosome at 5.5 Å resolution. Science *292*, 883–896.